Available online at www.sciencedirect.com

ScienceDirect

Biochimica et Biophysica Acta 1768 (2007) 2596–2604

Biochimica et Biophysica Acta BBA

www.elsevier.com/locate/bbamem

Domain formation by a *Rhodococcus* sp. biosurfactant trehalose lipid incorporated into phosphatidylcholine membranes

Francisco J. Aranda [a], José A. Teruel [a], María J. Espuny [c], Ana Marqués [c], Ángeles Manresa [c], Elisa Palacios-Lidón [b], Antonio Ortiz [a,*]

[a] *Departamento de Bioquímica y Biología Molecular-A, Facultad de Veterinaria, Universidad de Murcia, Campus de Espinardo, E-30100 Murcia, Spain*
[b] *Departamento de Física, Edificio CIOyN, Universidad de Murcia, Campus Espinardo, E-30100 Murcia, Spain*
[c] *Laboratorio de Microbiología, Facultad de Farmacia, Universidad de Barcelona, Joan XXIII s/n, E-08028 Barcelona, Spain*

Received 2 April 2007; received in revised form 25 May 2007; accepted 14 June 2007
Available online 23 June 2007

Abstract

The study of the interaction of biosurfactants with biological membranes is of great interest in order to gain insight into the molecular mechanisms of their biological actions. In this work we report on the interaction of a bacterial trehalose lipid produced by *Rhodococcus* sp. with phosphatidylcholine membranes. Differential scanning calorimetry measurements show a good miscibility of the glycolipid in the gel state and immiscibility in the fluid state, suggesting domain formation. These domains have been visualized and characterized, for the first time, by scanning force microscopy. Incorporation of trehalose lipid into phosphatidylcholine membranes produces a small shift of the antisymmetric stretching band toward higher wavenumbers, as shown by FTIR, which indicates a weak increase in fluidity. The C═O stretching band shows that incorporation of trehalose lipid increases the proportion of the dehydrated component in mixtures with the three phospholipids at temperatures below and above the gel to liquid–crystalline phase transition. This dehydration effect is also supported by data on the phospholipid P═O stretching bands. Small-angle X-ray diffraction measurements show that in the samples containing trehalose lipid the interlamellar repeat distance is larger than in those of pure phospholipids. These results are discussed within the frame of trehalose lipid domain formation, trehalose lipid/phospholipid interactions and its relevance to membrane-related biological actions.

Keywords: Biosurfactant; Trehalose lipid; Phospholipid membrane; Membrane domain

1. Introduction

The term biosurfactant has been widely applied to any amphiphilic compound of biological origin with the capacity of lowering the surface tension of water and aqueous solutions. Currently, biosurfactants are defined as surface-active compounds of microbial origin [1]. The great majority of compounds of this type reported in the literature are produced by bacteria, fungi or yeasts [2], and they have different natural roles [3]. From the chemical point of view biosurfactants present a wide structural diversity, the compounds with the most interesting properties being lipopeptides and glycolipids [1,2]. Biosurfactants are gaining an enormous interest because they show improved properties as compared to their chemically synthesized counterparts. As a general rule, biosurfactants are more biocompatible, more easily biodegradable, and therefore less toxic and less harmful with the environment, and more active at lower concentrations [1,2]. In addition, some of them display interesting biological activities [4]. Thus, applications of these compounds in several fields have been suggested [5–7], and the commercial production of biosurfactants has been encouraged in order to develop more economically attractive processes, including green biological processes [8–10]. In spite of these interesting properties, many of which are a result of their interaction with membranes, very few studies have been focused on the study of the molecular basis underlying their membrane-related biological actions. Surfactin, a biologically active lipopeptide biosurfactant produced by *Bacillus subtilis*, has been the subject of several works [11–14]. With respect to

* Corresponding author. Tel.: +34 968 364788; fax: +34 968 364147.
E-mail address: ortizbq@um.es (A. Ortiz).

0005-2736/$ - see front matter © 2007 Elsevier B.V. All rights reserved.
doi:10.1016/j.bbamem.2007.06.016

glycolipids, rhamnolipids secreted by *Pseudomonas aeruginosa* are by far the most actively studied. Several recent works have shown the effects of these interesting compounds on phospholipid membranes of various compositions [15–18]. Another group of glycolipid biosurfactants is formed by trehalose-containing glycolipids [19]. These trehalose lipids are mainly produced by rhodococci and present interesting physicochemical and biological properties [20]. Trehalose lipids, with a reported CMC in the range of 0.02–0.17 g/l [21], significantly reduce the surface tension of water [22], and form microemulsions [23]. Thus, a number of possible applications for these compounds have been proposed [20]. This work presents a biophysical approach to the study of the interactions of a *Rhodococcus* trehalose lipid with model membranes made of phosphatidylcholines of various acyl chain lengths, in order to get insight into the molecular mechanism of the modulation of membrane physical organization by this biosurfactant.

2. Materials and methods

2.1. Materials

1-Palmitoyl-2-oleoylphosphatidylcholine (POPC), dimyristoylphosphatidylcholine (DMPC), dipalmitoylphosphatidylcholine (DPPC) and distearoylphosphatidylcholine (DSPC) were purchased from Avanti Polar Lipids Inc. (Birmingham, AL). All the other reagents were of the highest purity available. Purified water was deionised in a Milli-Q equipment from Millipore (Bedford, MA), and filtered through 0.24 μm filters prior to use. Stock solutions of the various phosphatidylcholines and the trehalose lipid were prepared in chloroform/methanol (1:1) and stored at −20 °C. Phospholipid concentrations were determined by phosphorous analysis [24].

2.2. Trehalose lipid production and purification

Strain 51T7 was isolated from an oil-contaminated soil sample after culture enrichment with kerosene, and was identified as *Rhodococcus* sp. [25]. This strain was maintained by fortnightly cultures on Trypticase Soy Agar (Pronadisa, Spain) and preserved in cryovials at −20 °C. Biosurfactants were produced, purified and characterized as described before [21,25,26]. Trehalose lipids were found to be >95% pure by thin-layer chromatography on silica gel plates, using chloroform/methanol/H_2O (65:15:2) as mobile phase and H_2SO_4 staining. The glycolipid contained succinic, heptanoic, decanoic, nonanoic and undecanoic acids, as determined before by GC [25].

2.3. Differential scanning calorimetry measurements

Samples for DSC were prepared by mixing the appropriate amounts of phospholipid and trehalose lipid in chloroform/methanol (1: 1). The solvent was gently evaporated under a stream of dry N_2 to obtain a thin film at the bottom of a small glass tube. Last traces of solvent were removed by a further 2-h desiccation under high vacuum. To the dry samples, 50 μl of a buffer containing 150 mM NaCl, 0.1 mM EDTA, 10 mM HEPES pH 7.4 was added, and vesicles were formed by vortexing the mixture, always keeping the temperature above the highest gel to liquid–crystalline phase transition of the sample, i.e. 35 °C in the case of DMPC, 50 °C for DPPC and 60 °C for DSPC. 15 μl of the vesicle suspensions was sealed in small aluminium calorimetry pans and scanned. Scans were carried out in a Perkin-Elmer DSC-7 equipment, at heating and cooling rates of 4 °C min^{-1}. The calorimeter was calibrated using the pure phospholipids as standards.

Partial phase diagrams for the phospholipid component were constructed from the heating thermograms. The *solidus* and *fluidus* lines of the diagrams were defined by the onset and completion temperatures of the transition peaks obtained from heating scans. In order to avoid artifacts due to the thermal history of the sample the first scan was never considered. Second and further scans were carried out until a reproducible and reversible pattern was obtained, what usually occurred already with the second scan. The pretransitions were omitted from the diagrams for the sake of simplicity.

2.4. Small angle X-ray diffraction measurements

Samples for X-ray diffraction analysis were prepared essentially as described above for DSC. The lipid suspensions were placed in a steel holder, which provided good thermal contact to the Peltier heating unit, with cellophane windows. Typical exposure times were 5 min, allowing 10 min prior to the measurement for temperature equilibration.

Small angle X-ray diffraction (SAXD) measurements were carried out using a Kratky compact camera (MBraum-Graz-Optical Systems, Graz, Austria) and a linear position sensitive detector (PSD; MBraum, Garching, Germany) monitoring the s-range ($s=2\sin\theta/\lambda$, 2θ=scattering angle, $\lambda=1.54$ Å) between 0.0075 and 0.07 $Å^{-1}$. Nickel-filtered Cu K_α X-rays were generated by a Philips (Eindhoven, The Netherlands) PW3830 X-ray generator operating at 50 kV and 30 mA. The calibration of the detector position was performed by using silver stearate (d-spacing at 48.8 Å) as reference material.

2.5. Fourier transform infrared spectroscopy measurements

For the infrared measurements multilamellar vesicles were prepared, as described above, in 50 μl of the same buffer prepared in D_2O. Samples were placed between two CaF_2 windows (25×2 mm) separated by 50 μm Teflon spacers and mounted in a thermostated Symta cell holder. Infrared spectra were acquired in a Nicolet MX-1 Fourier-transform infrared spectrometer (FTIR) (Madison, WI), provided with computer data collection. Each spectrum was obtained by collecting 27 interferograms. The D_2O buffer spectrum taken at the same temperature was subtracted interactively using GRAMS/32 as described previously [12].

2.6. Scanning force microscopy

For the scanning force microscopy (SFM) measurements small unilamellar vesicles (SUV) of the appropriate composition were prepared by probe sonication of multilamellar vesicles as described before [18]. Supported bilayers were obtained by deposition of a drop of the SUV sample on top of a fresh cleaved round mica dish and incubation for 30 min at room temperature. The samples were finally washed 20 times with buffer, and the bottom of the mica dish was dried with tissue paper.

SFM experiments were performed at room temperature and ambient conditions using a Nanotec Electronica (Madrid, Spain) SFM system with a PLL/dynamic measurement board. Topography images were acquired working in amplitude modulation non-contact dynamic mode with silicon tetrahedral tips (Olympus Optical Co. LDT, OMCL-AC series, long cantilevers (length 240 μm), nominal force constant 2 N/m, resonance frequency 70 kHz). Relatively small oscillation amplitudes (10 nm peak-peak) and a small reduction of oscillation amplitude were used (about 90% of the free oscillation amplitude). The phase locked loop of our dynamic measurement board was enabled to keep the tip sample system always at resonance. In this way, measurements were done in the attractive regime of tip-sample interaction without touching the surface.

3. Results and discussion

The marked amphiphilic character of the trehalose lipid biosurfactant, with a hydrophobic part formed by the fatty acyl chains, and a hydrophilic portion that contains the sugar rings (Fig. 1), is expected to result in strong interactions with the phospholipid constituents of membrane bilayers. In the present work the interaction of trehalose lipid with phosphatidylcholine membranes has been studied, in order to get insight into the localization of the glycolipid into the phospholipid bilayer and its effect on membrane structure. We have evaluated, by means

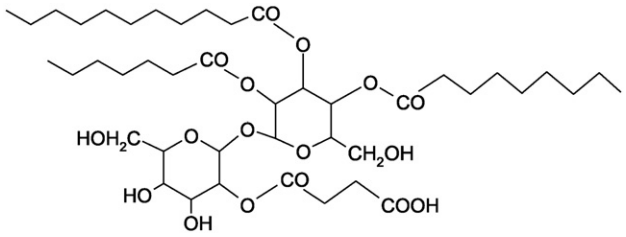

Fig. 1. The chemical structure of *Rhodococcus* sp. trehalose lipid.

of DSC, SFM, FTIR and X-ray diffraction, the effect of phospholipid acyl chain length on trehalose lipid/phospholipid interactions.

3.1. Domain formation in trehalose lipid/phosphatidylcholine membranes

Fig. 2 shows the DSC profiles of mixtures of trehalose lipid with three phosphatidylcholines that differ in the hydrocarbon chain length, namely DMPC (panel A), DPPC (panel B) and DSPC (panel C). First of all it should be pointed out that pure trehalose lipid suspensions, at concentrations of the same order that those of the phospholipids, did not exhibit any thermotropic transition in the range of −12 to 70 °C (not shown). Therefore all the transitions shown must be attributed to the phospholipids. Increasing the trehalose lipid concentration in DMPC (Fig. 2A) progressively made the pretransition smaller, which was completely abolished at 3 mol%. The main gel to liquid–crystalline phase transition was progressively broadened and shifted to lower temperatures as the concentration of trehalose lipid was increased. At 7 mol% of trehalose lipid, a second peak above the main transition became apparent, and was more prominent as the concentration of the glycolipid was increased. Thus, at 10 mol% trehalose lipid two well-differentiated transitions were clearly observed. These new peaks must be due to mixed phases since the pure trehalose lipid did not shown any thermotropic transition in this range as explained above. At the maximum concentration of trehalose lipid assayed (30 mol %) a very broadened transition was still present. The pattern observed for DPPC and DSPC bilayers (Fig. 2B and C) was qualitatively similar, also with respect to the appearance of new peaks, and indicated a lateral segregation of different phases within the plane of the bilayer.

From the calorimetric data obtained from the scans shown in Fig. 2 partial phase diagrams for the phospholipid component were constructed (Fig. 3). For the sake of simplicity the pretransitions were omitted from the phase diagrams. The partial phase diagrams for DMPC and DPPC (Fig. 3A and B) indicated a near-ideal behavior for the *solidus* line, which shifted to lower temperatures as the concentration of trehalose lipid was increased. In the diagram for DMPC (Fig. 3A) the *fluidus* line slightly increased with trehalose lipid concentration, indicating that fluid-phase immiscibility was taking place for all the trehalose lipid concentrations examined. Thus, in the region defined by G+F at least two fluid phases should coexist with the gel phase, since two peaks were observed in the thermograms at trehalose lipid concentrations above 7 mol% (Fig. 2A). A similar immiscibility was observed for the mixtures with DPPC, since the *fluidus* line remained horizontal for the whole concentration range (Fig. 3B). The phase diagram for the system trehalose lipid/DSPC (Fig. 3C) did not share the characteristics of the other two phospholipids, since both the *solidus* and the *fluidus* lines decreased with increasing trehalose lipid concentrations, indicating good miscibility both in the gel and the liquid–crystalline state and a near-ideal behavior for the system formed by these two lipids. Nevertheless the effect on the *fluidus* line was very weak. These results indicated that trehalose lipid interactions, for the C_{16} and C_{14} acyl chains of DPPC and DMPC, led to domain formation. Domain formation has been shown before in the case of other biosurfactants, thus surfactin [12] and dirhamnolipid [16] also

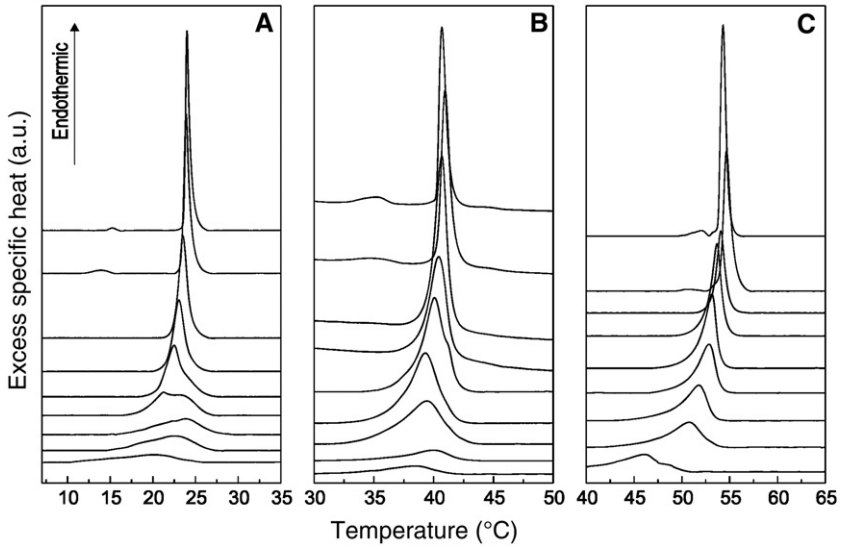

Fig. 2. DSC heating-scan thermograms for mixtures of trehalose lipid with DMPC (A), DPPC (B) and DSPC (C). Each sample contained 2 μmol phospholipid and 0, 1, 3, 5, 7, 10, 15, 20 and 30 mol% of trehalose lipid (from top to bottom).

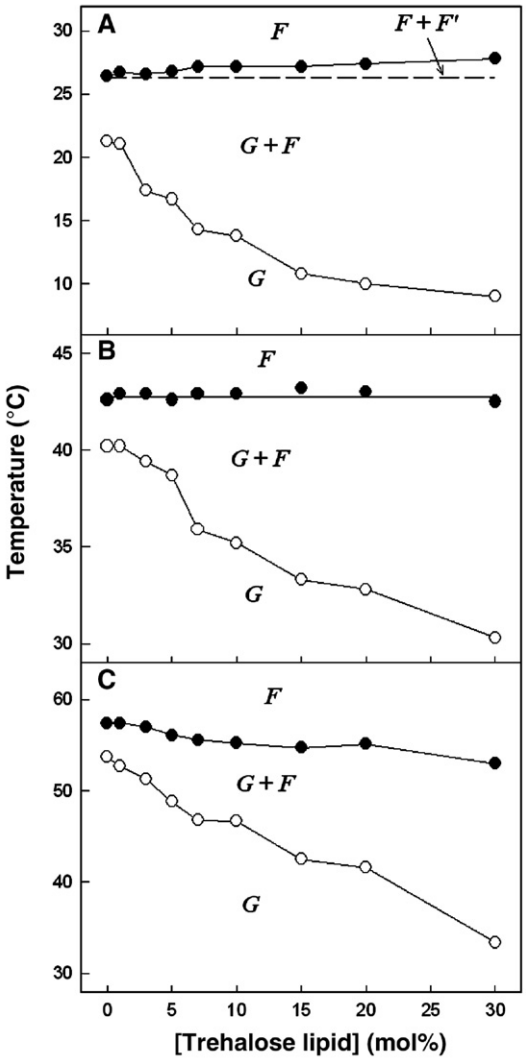

Fig. 3. Partial phase diagrams for mixtures of trehalose lipid with DMPC (A), DPPC (B) and DSPC (C). Open symbols represent the *solidus* line and filled symbols represent the *fluidus* line. G corresponds to a lamellar L_β gel phase and F and F′ to lamellar L_α fluid phases (see text for explanation).

presented fluid immiscibility in mixtures with DMPC, which was suggested to be behind their membrane permeabilization activity [13].

The interaction of trehalose lipid with POPC was qualitatively similar, according to the DSC results (Fig. 4). In this case the effects were stronger than in the case of saturated phosphatidylcholines since phase separation was already observed at just 1 mol% of trehalose lipid (Fig. 4A). Increasing the concentration of the glycolipid progressively broadened and shifted the transition to lower temperatures. The lower melting peak was progressively diminished in favor of the higher melting one, which was the only present at 7 mol%. The corresponding partial phase diagram (Fig. 4B) also showed fluid-phase immiscibility within this concentration range, as described above for saturated phosphatidylcholines. A stronger interaction with unsaturated phosphatidylcholines versus saturated ones was also described before for mixture of α-tocopherol various phosphatidylcholines [27].

In order to visualize trehalose lipid domains, the topology of supported bilayers was examined by means of SFM (Fig. 5). For these experiments the membranes were prepared with POPC which is in the fluid state at room temperature. For pure POPC samples (Fig. 5A) the mica was almost completely covered, indicating good fusion of SUV above the mica sheet. Only a few holes were present, probably produced during the drying process. The horizontal line profile at position 1 (Fig. 5, panel 1) showed that bilayer thickness was 6±1 nm. In some areas two or even three stacked bilayers could be observed. The topographic images showed that in all the regions the bilayers were homogeneous. In the samples containing trehalose lipid (Fig. 5B), the holes which were present in the pure POPC sample were not found. However, since the characteristic features of a mica surface were not observed, it was possible to conclude that the mica surface was again completely covered

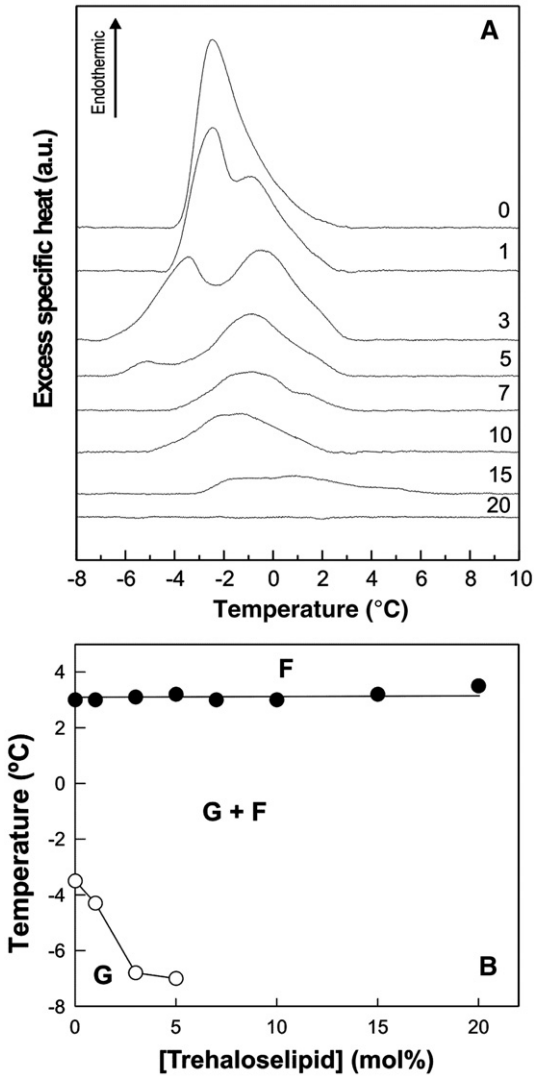

Fig. 4. DSC heating-scan thermograms for mixtures of trehalose lipid with POPC (panel A). Each sample contained 2 μmol phospholipid and the concentration of trehalose lipid (mol%) indicated on the curves. Panel B: partial phase diagram obtained from the thermograms shown in panel A. Open symbols represent the *solidus* line and filled symbols the *fluidus* line. G corresponds to a lamellar L_β gel phase and F to lamellar L_α fluid phase (see text for explanation).

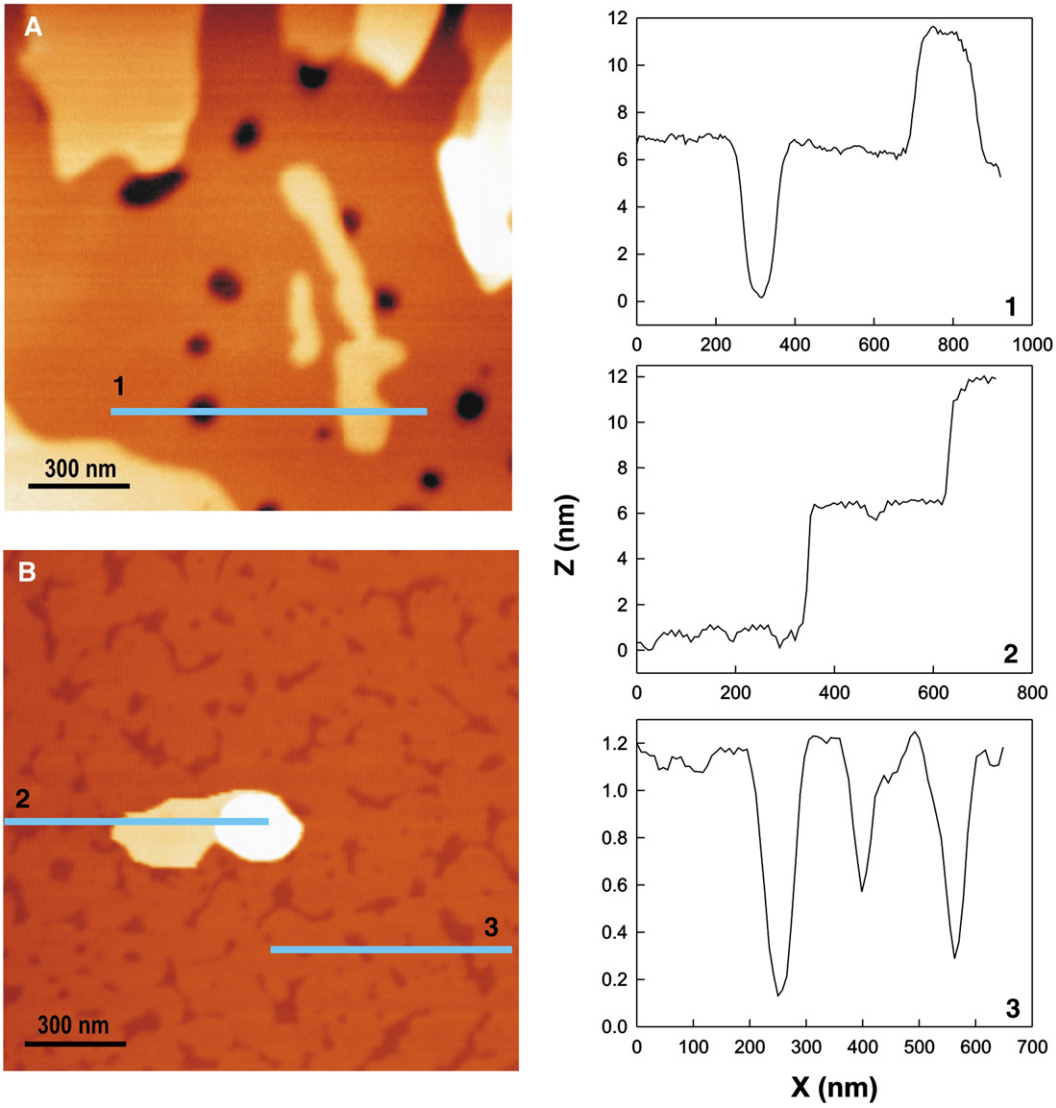

Fig. 5. Topology of pure POPC supported bilayers (panel A) and POPC/trehalose lipid 20 mol% supported bilayers (panel B) as visualized by SFM. The samples were prepared and scanned at 25 °C. Plots 1, 2 and 3 on the right correspond to the horizontal cross sections at the indicated positions in panels A and B. Note the much smaller height scale of profile 3 (1.2 nm) as compared to profiles 1 and 2 (12 nm).

with a bilayer. In these samples the bilayer surface was not homogeneous as in the pure POPC sample but two different domains with irregular size and shape were evident. Examination of the profile at position 3 (Fig. 5, panel 3) showed that the height difference between the two domains was about 1 ± 0.3 nm, indicating that the trehalose lipid tends to form domains within the POPC matrix. In some regions two or even three stacked bilayer, with a thickness of 6 ± 1 nm, were occasionally observed. We note that this latter height corresponds to the POPC bilayer thickness, and is much higher than the difference between the domains in a single layer. According to the cross section profile shown in panel 2, the domains structure, characteristic of these composed bilayers were present not only in the bottom bilayer but also in the first and second stacked ones. Taken together, our DSC and SFM results have unequivocally shown domain formation by a bacterial biosurfactant in a phospholipid bilayer. Quantitative determination of the proportion of domains by image analysis yielded a value close to 20%, indicating, in conjunction with the DSC data, that the domains were essentially formed by pure trehalose lipid. This is the first time that these types of domains, formed by a bacterial biosurfactant, have been visualized by SFM. This segregation of trehalose lipid within the plane of the bilayer indicated that self-interaction prevailed over interaction with the phospholipid molecules, which could be important to explain the membrane-related activities of the biosurfactant.

3.2. Fourier-transform infrared spectroscopy

The molecular interactions of trehalose lipid with the different parts of the phospholipid molecules, basically the polar region (C═O and P═O stretching bands) and the acyl chains (–CH_2– stretching bands) were investigated by FTIR.

The C═O groups of diacylphospholipids in lipid vesicles may be in a hydrated and a dehydrated state, their proportion depending on the physical state of the phospholipid bilayer

[28,29]. The spectrum of a pure phospholipid represents a summation of two component bands centered near 1742 and 1727 cm^{-1}, and attributed to dehydrated and hydrated C═O groups, respectively [30]. Fig. 6A shows that the C═O stretching band of pure DPPC at 25 °C (gel phase), centered at ca. 1732 cm^{-1}, was shifted to ca. 1738 cm^{-1} upon addition of 15 mol% trehalose lipid. Qualitatively similar results were obtained with phospholipids in the fluid phase, as well as for the mixtures with the other phospholipids. This shift already suggested a dehydration effect of the glycolipid. It has to be taken into consideration that pure trehalose lipid also presented a C═O stretching absorption in this region (Fig. 6A) which, even though its concentration was just 15 mol%, could modify the results to a certain extent. The spectra of the various trehalose lipid/phospholipid systems were fitted using a Gaussian–Lorentzian function, and the proportions of the dehydrated and hydrated components were calculated. It was observed that incorporation of just 5 mol% of trehalose lipid increased the proportion of the dehydrated component in mixtures with the three phospholipids at temperatures below and above the gel to liquid–crystalline phase transition. A further increase in the concentration of the glycolipid to 15 mol % resulted in a considerable larger proportion of the dehydrated component (up to 40%), which interestingly was substantially higher in the gel phase than in the fluid phase. These results indicated that trehalose lipid interacted with the polar region of the bilayer decreasing hydrogen bonding of the phospholipid C═O groups with the water molecules of the hydration layer. Probably trehalose lipid, bearing a large number of free hydroxyl groups, will itself participate in a high number of hydrogen bonds, thus leaving less water molecules available for interacting with the phospholipid. The stronger effect observed when the phospholipids were in the gel phase must be due to the fact that, under these conditions, the trehalose lipid was near-ideally mixed with the phospholipid, whereas the lateral segregation of the glycolipid due to the fluid phase immiscibility shown above resulted in a considerable reduction of its interactions with the phospholipid molecules.

Another infrared absorptions which are sensitive to hydration are the P═O stretching bands. Phospholipids present two strong bands around 1250 and 1085 cm^{-1} due to the P═O stretching (antisymmetric and symmetric respectively) [31]. In principle, these bands should be useful to study trehalose lipid/phospholipid interactions since the glycolipid does not present these vibrations. However, as shown in Fig. 7, pure trehalose lipid also presented a strong absorption band in the same position that the antisymmetric P═O stretching, and a small one in the zone of the symmetric P═O stretching, which are due to C–O stretching of the trehalose sugar rings [32]. However, the symmetric P═O stretching band should be a better choice since it is less affected by the trehalose lipid C–O stretching than the antisymmetric one. Thus, in Fig. 7 it can be observed that the symmetric P═O stretching band of pure DPPC (1092 cm^{-1}) was shifted to lower values (1088 cm^{-1}) and its intensity was reduced upon incorporation of trehalose lipid. The fact that the P═O stretching was diminished in intensity by effect of trehalose lipid already suggested major changes occurring in this band, and the displacement to lower values indicated a dehydration effect, confirming the results discussed above from the C═O stretching. A similar effect was shown before for the interaction of trehalose with DPPC [32], even though the two systems may be very different since in the case of trehalose lipid trehalose is tethered to the bilayer. Goodrich et al. [33] also described hydrogen bonding between

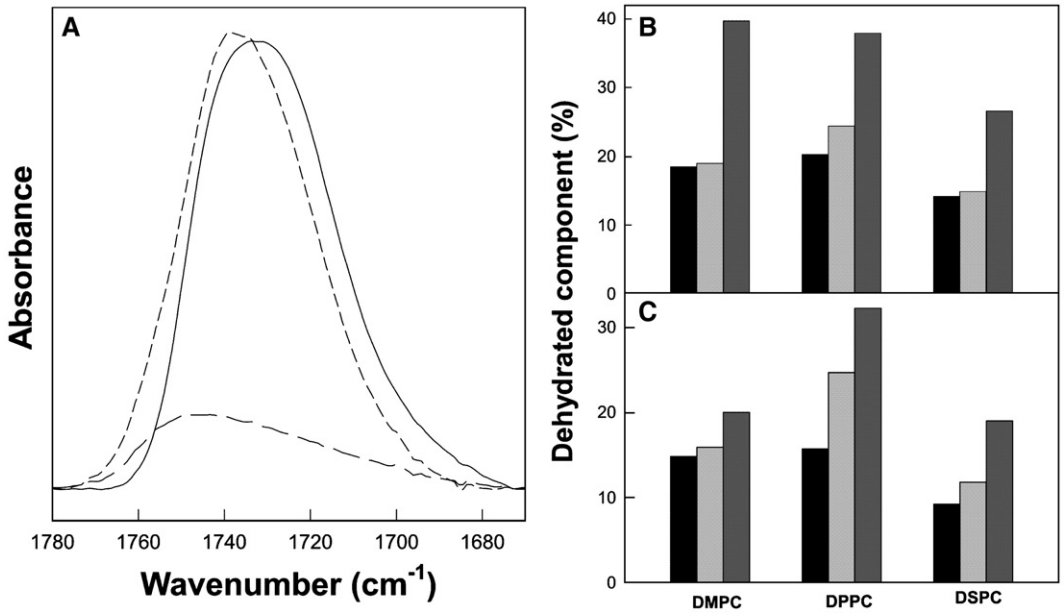

Fig. 6. FTIR spectra in the region of C═O stretching band for pure DPPC (solid line), DPPC containing 15 mol% trehalose lipid (short-dashed line) and pure trehalose lipid (long-dashed line), at 25 °C (panel A). Panel B: relative area of the dehydrated component of the carbonyl stretching band of DMPC, DPPC and DSPC in the gel L_β phase. Panel C: relative area of the dehydrated component of the carbonyl stretching band of DMPC, DPPC and DSPC in the fluid L_α phase. The results correspond to the pure phospholipid (black) and mixtures containing 5 mol% (light grey) and 15 mol% (dark grey) trehalose lipid.

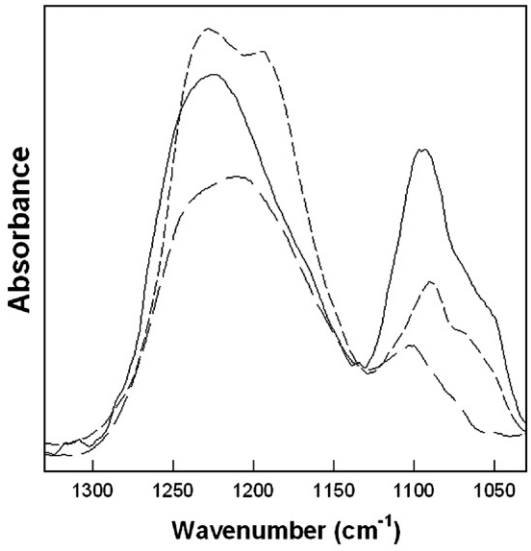

Fig. 7. FTIR spectra in the region of the symmetric (ca. 1085 cm^{-1}) and antisymmetric (ca. 1250 cm^{-1}) P═O stretching bands for pure DPPC (solid line), DPPC containing 15 mol% trehalose lipid (short-dashed line) and pure trehalose lipid (long-dashed line). The measurements were carried out at 25 °C.

maltose coupled to cholesterol and DPPC bilayers, very similar to the results we have shown here.

Fig. 8 shows the characteristic $–CH_2–$ stretching bands of pure DPPC and trehalose lipid, and a 15-mol % mixture at 25 °C. Both DPPC and trehalose lipid showed the same vibrations, but the intensity was apparently diminished in the case of the glycolipid. Incorporation of trehalose lipid into DPPC shifted the maxima of the bands to higher values. The other phospholipids presented similar spectra in this region. Table 1 shows the frequencies of the $–CH_2–$ stretching bands of DMPC, DPPC and DSPC, in the absence and presence of trehalose lipid, both below and above the gel to liquid–crystalline phase transition. The incorporation of up to 15 mol%

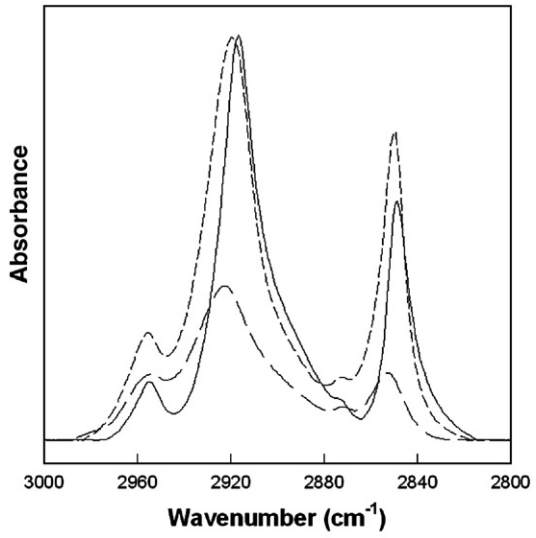

Fig. 8. FTIR spectra of the $–CH_2–$ stretching absorption bands of pure DPPC (solid line), DPPC containing 15 mol% trehalose lipid (short-dashed line) and pure trehalose lipid (long-dashed line), at 25 °C.

Table 1
Effect of trehalose lipid on the antisymmetric (2916 cm^{-1}) and symmetric (2848 cm^{-1}) stretching bands of the C═O groups of various phosphatidylcholines

Sample	Wavenumber (cm^{-1})			
	Gel phase		Liquid–crystalline phase	
	Antisymmetric	Symmetric	Antisymmetric	Symmetric
DMPC	2915.6	2848.1	2919.1	2849.9
DMPC+5 mol% TL	2917.2	2849.4	2919.7	2851.3
DMPC+15 mol% TL	2917.7	2849.6	2921.3	2851.7
DPPC	2916.1	2848.6	2920.1	2850.7
DPPC+5 mol% TL	2916.8	2849.2	2921.9	2851.5
DPPC+15 mol% TL	2917.3	2849.6	2921.6	2851.8
DSPC	2917.4	2849.2	2921.1	2851.6
DSPC+5 mol% TL	2917.3	2849.7	2922.1	2852.1
DSPC+15 mol% TL	2918.2	2849.7	2922.2	2852.5

of trehalose lipid produced a small shift of the antisymmetric stretching band (around 2916 cm^{-1}) toward higher wavenumbers in mixtures with the three phospholipids, both below and above the phase transition, which indicated a weak increase in fluidity, in agreement with the DSC results. The effect on the symmetric stretching band (around 2848 cm^{-1}) was even weaker. These displacements were much smaller than those observed in the pure phospholipids as a consequence of the gel to liquid–crystalline phase transition, which were about 4 cm^{-1}, indicating that the interaction of the trehalose lipid with the phospholipid acyl chains was weak, as suggested above, and did not result in a large additional disordering of the acyl chain region of the fluid bilayer.

3.3. X-ray diffraction

The effect of incorporation of trehalose lipid on the phase adopted by the membrane and its properties was studied in mixtures of trehalose lipid with DMPC, DPPC and DSPC, by performing small-angle X-ray diffraction (SAXD) and wide-angle X-ray diffraction (WAXD) experiments. When phospholipids organize into multilamellar structures give rise to SAXD reflections which positions relate as 1:1/2:1/3:1/4... [34]. Fig. 9 shows the SAXD diffraction profiles of pure phosphatidylcholines and their mixtures with trehalose lipid at temperatures below and above the gel-to-liquid crystalline phase transition of each pure phospholipid. Pure DMPC showed three reflections with relative distances of 1:1/2:1/3, whereas for DPPC and DSPC up to six reflections which related as 1:1/2:1/3:1/4:1/5 could be observed, which was consistent with their organization in multilamellar structures. The addition of 5 mol% of trehalose lipid did not change the lamellar organization of the three phosphatidylcholine species, but the reflections lose sharpness and intensity. At 15 mol% this effect was very intense, with the presence of wide scattering bands that indicated a large reduction of long-range structural order in the three lamellar systems. SAXD also allows the determination of the interlamellar repeat distance, d, in the lamellar phase. The largest first-order reflection component corresponds to the interlamellar repeat distance which is comprised of the bilayer thickness and the thickness of one adjacent interlamellar water layer [35]. As

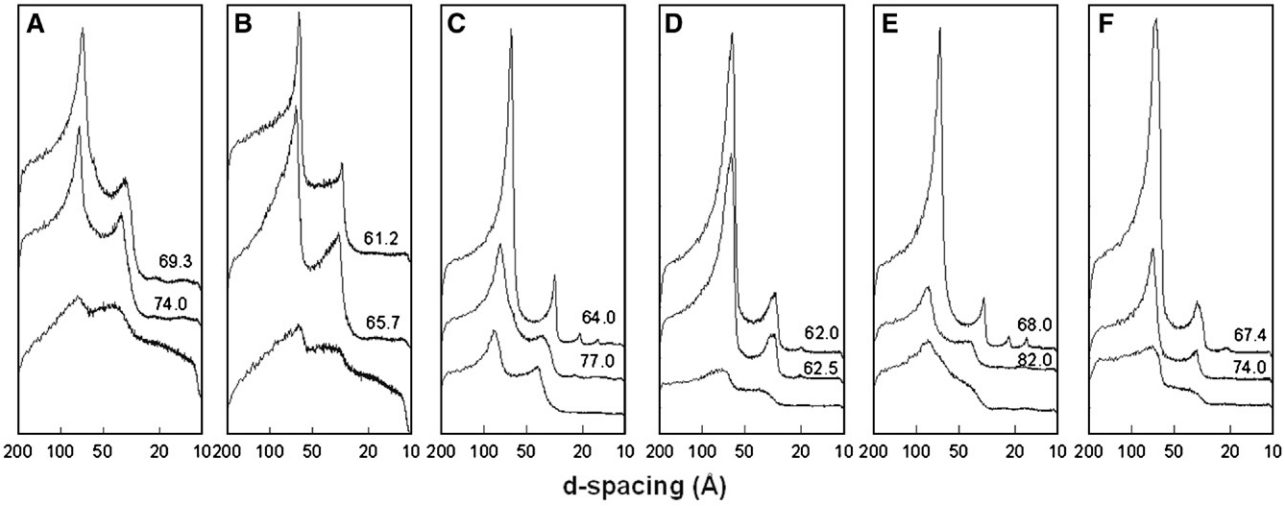

Fig. 9. Small-angle X-ray diffraction patterns of various phosphatidylcholines and mixtures with trehalose lipid. (A) DMPC in the gel phase (15 °C), (B) DMPC in the fluid phase (35 °C), (C) DPPC in the gel phase (25 °C), (D) DPPC in the fluid phase (50 °C), (E) DSPC in the gel phase (30 °C) and (F) DSPC in the fluid phase (60 °C). The three profiles shown in each panel correspond, from top to bottom, to pure phospholipid, phospholipid containing 5 mol% trehalose lipid, and phospholipid containing 15 mol% trehalose lipid. The numbers on the profiles are the corresponding value of the interlamellar repeat distances, *d*.

shown in Fig. 9A and B DMPC gave rise to a first-order reflection with a *d*-value of 69.3 Å in the gel state and 61.2 Å in the liquid crystalline state. For DPPC the *d*-values in the gel and liquid crystalline state were 64.0 and 62.0 Å respectively (Fig. 9C and D), and 68.0 and 67.4 Å respectively for DSPC (Fig. 9E and F). In the samples containing 5 mol% of trehalose lipid the interlamellar repeat distance *d* was found to be between 4 and 14 Å (depending on acyl chain and temperature) larger than those of the pure phospholipids (Fig. 9A), which must be the result of an effective increase of the bilayer thickness, as discussed below, or the thickness of the hydration layer between bilayers. This latter effect can be due to an increase in hydrogen bonding due to the presence of the large number of hydroxyl groups of the glycolipid, as discussed above. The wide scattered bands present at 15 mol% trehalose lipid (Fig. 9) did not allow the precise determination of *d*-spacing values at this glycolipid concentration.

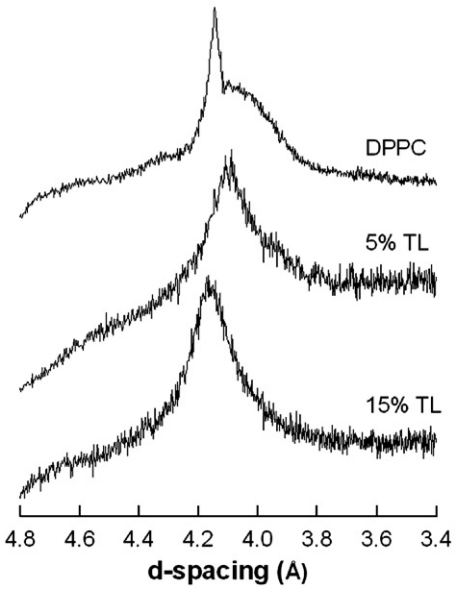

Fig. 10. Wide-angle X-ray diffraction profiles for pure DPPC, and DPPC containing 5 mol% and 15 mol% trehalose lipid (from top to bottom). The measurements were carried out at 25 °C, i.e., with DPPC in the gel phase.

Measurements in the wide-angle region (WAXD) provide information about the packing of the phospholipids acyl chains. Fig. 10 shows the WAXD pattern corresponding to pure DPPC and DPPC containing 5 and 15 mol% trehalose lipid at 25 °C, i.e., in the gel phase. Pure DPPC showed a sharp reflection at 4.19 Å surrounded by a broad reflection around 4.10 Å, which was typical for lipid bilayers in the lamellar gel phase with tilted hydrocarbon chains and pseudohexagonal chain packing [36]. In the presence of trehalose lipid, the sharp reflection with its shoulder was replaced by a rather symmetric reflection around 4.14 Å, indicating that the hydrocarbon chains were oriented perpendicular to the bilayer plane, which was in accordance with an untilting of the acyl chains [37]. This untilting of the phospholipid acyl chains also contributed to explain the increase in the interlamellar repeat distance shown above from SAXD data. The effect of trehalose lipid on acyl chain packing, when incorporated into DMPC or DSPC systems, was similar to that commented above for the DMPC system (not shown). These results indicated that trehalose lipid was able to perturb the packing of the phosphatidylcholine acyl chains and that this perturbation did not depend on acyl chain length.

4. Conclusions

The intent of this work was to characterize the interactions of a trehalose lipid bacterial biosurfactant with membranes composed of phosphatidylcholines of different acyl chain length. Our results have demonstrated that trehalose lipid segregates into domains when incorporated into fluid phosphatidylcholine membranes. These biosurfactant domains into a phospholipid membrane have been visualized and characterized, for the first time, by SFM. The molecular interactions observed

for trehalose lipid and phosphatidylcholine, both below and above the gel to liquid–crystalline phase transition, can be summarized as a small increase in fluidity and a large dehydration of the polar region of the membrane, together with an effective increase of the interlamellar repeat distance, *d*. This increase of *d* can be the result of increased hydrogen bonding, of an effective increase of bilayer thickness due to untilting of the phospholipid acyl chains, or both. The described interactions would probably result in an alteration of bilayer stability, and in this respect we have previous indications that trehalose lipid is able to permeabilize phospholipid membranes, studies which will be the subject of a future work. Since trehalose lipid, like most known biosurfactants, present a wide variety of biological actions, including effects on biological membranes [4], our results are aimed to explain the molecular interactions underlying these effects.

Acknowledgement

This work was financially supported by Project CTQ2004-00107 (to A.O.) from Ministerio de Ciencia y Tecnología, Spain.

References

[1] S. Lang, Biological amphiphiles (microbial biosurfactants), Curr. Opin. Colloid Interface Sci. 7 (2002) 12–20.
[2] E. Rosenberg, E.Z. Ron, High- and low-molecular-mass microbial surfactants, Appl. Microbiol. Biotechnol. 52 (1999) 154–162.
[3] E.Z. Ron, E. Rosenberg, Natural roles of biosurfactants, Environ. Microbiol. 3 (2001) 229–236.
[4] S. Lang, F. Wagner, Biological activities of biosurfactants, in: N. Kosaric (Ed.), Biosurfactants, vol. 48, Dekker, New York, 1993, pp. 251–258.
[5] P. Singh, S.S. Cameotra, Potential applications of microbial surfactants in biomedical sciences, Trends Biotechnol. 22 (2004) 142–146.
[6] S.S. Cameotra, R.S. Makkar, Recent applications of biosurfactants as biological and immunological molecules, Curr. Opin. Microbiol. 7 (2004) 262–266.
[7] L. Rodrigues, I.M. Banat, J. Teixeira, R. Oliveira, Biosurfactants: potential applications in medicine, J. Antimicrob. Chemother. 57 (2006) 609–618.
[8] J.D. Desai, I.M. Banat, Microbial production of surfactants and their commercial potential, Microbiol. Mol. Biol. Rev. 61 (1997) 47–64.
[9] R.S. Makkar, S.S. Cameotra, An update on the use of unconventional substrates for biosurfactant production and their new applications, Appl. Microbiol. Biotechnol. 58 (2002) 428–434.
[10] S. Mukherjee, P. Das, R. Sen, Towards commercial production of microbial surfactants, Trends Biotechnol. 24 (2006) 509–515.
[11] R. Maget-Dana, M. Ptak, Interactions of surfactin with membrane models, Biophys. J. 68 (1995) 1937–1943.
[12] A. Grau, J.C. Gómez-Fernández, F. Peypoux, A. Ortiz, A study of the interactions of surfactin with phospholipid vesicles, Biochim. Biophys. Acta 1418 (1999) 307–319.
[13] C. Carrillo, J.A. Teruel, F.J. Aranda, A. Ortiz, Molecular mechanism of membrane permeabilization by the peptide antibiotic surfactin, Biochim. Biophys. Acta 1611 (2003) 91–97.
[14] H. Heerklotz, T. Wieprecht, J. Seelig, Membrane perturbation by the lipopeptide surfactin and detergents as studied by deuterium NMR, J. Phys. Chem., B 108 (2004) 4909–4915.
[15] M. Sánchez, J.A. Teruel, M.J. Espuny, A. Marqués, F.J. Aranda, A. Manresa, A. Ortiz, Modulation of the physical properties of dielaidoylphosphatidylethanolamine membranes by a dirhamnolipid biosurfactant produced by *Pseudomonas aeruginosa*, Chem. Phys. Lipids 142 (2006) 118–127.
[16] A. Ortiz, J.A. Teruel, M.J. Espuny, A. Marqués, A. Manresa, F.J. Aranda, Effects of dirhamnolipid on the structural properties of phosphatidylcholine membranes, Int. J. Pharm. 325 (2006) 99–107.
[17] M. Sánchez, F.J. Aranda, M.J. Espuny, A. Marqués, J.A. Teruel, A. Manresa, A. Ortiz, Aggregation behaviour of a dirhamnolipid biosurfactant secreted by *Pseudomonas aeruginosa* in aqueous media, J. Colloid Interface Sci. 307 (2006) 246–253.
[18] F.J. Aranda, M.J. Espuny, A. Marqués, J.A. Teruel, A. Manresa, A. Ortiz, Thermodynamics of interaction of a dirhamnolipid biosurfactant secreted by *Pseudomonas aeruginosa* with phospholipid membranes, Langmuir 23 (2007) 2700–2705.
[19] C. Asselineau, J. Asselineau, Trehalose-containing glycolipids, Prog. Chem. Fats Other Lipids 16 (1978) 59–99.
[20] S. Lang, J.C. Philp, Surface-active compounds in rhodococci, Antonie Van Leeuwenhoek 74 (1998) 59–70.
[21] M. Martín, P. Bosch, J.L. Parra, M.J. Espuny, A. Virgili, Structure and bioconversion of trehalose lipids, Carbohydr. Res. 220 (1991) 93–100.
[22] B.A. Ramsay, D.G. Cooper, A. Margaritis, J.E. Zajic, Rodochrous bacteria: biosurfactant production and demulsifying ability, in: J.E. Zajic, D.G. Cooper, T.R. Jack, N. Kosaric (Eds.), Microbial enhanced oil recovery, PennWell Books, Tulsa, Oklahoma, 1983, pp. 61–65.
[23] M.E.V. Singer, W.R. Finnerty, A. Tunelid, Physical and chemical properties of a biosurfactant synthesized by Rhodococcus species H13-A, Can. J. Microbiol. 36 (1990) 746–750.
[24] C.J.F. Böttcher, C.M. Van Gent, C. Pries, A rapid and sensitive sub-micro phosphorus determination, Anal. Chim. Acta 24 (1961) 203–204.
[25] M.J. Espuny, S. Egido, M.E. Mercadé, A. Manresa, Characterization of trehalose tetraester produced by a waste lube oil degrader Rhodococcus sp. 51T7, Toxicol. Environ. Chem. 48 (1995) 83–88.
[26] M.J. Espuny, S. Egido, I. Rodón, A. Manresa, M.E. Mercadé, Nutritional requirements of a biosurfactant producing strain Rhodococcus sp 51T7, Biotechnol. Lett. 18 (1996) 521–526.
[27] M.P. Sánchez-Migallón, F.J. Aranda, J.C. Gómez-Fernández, Interaction between α-tocopherol and heteroacid phosphatidylcholines with different amounts of unsaturation, Biochim. Biophys. Acta 1279 (1996) 251–258.
[28] A. Blume, W. Hübner, G. Messner, Fourier transform infrared spectroscopy of 13C═O-labeled phospholipids hydrogen bonding to carbonyl groups, Biochemistry 27 (1998) 8239–8249.
[29] R.N.A.H. Lewis, R.N. McElhaney, W. Pohle, H.H. Mantsch, Components of the carbonyl stretching band in the infrared spectra of hydrated 1,2-diacylglycerolipid bilayers: a reevaluation, Biophys. J. 67 (1994) 2367–2375.
[30] H.H. Mantsch, R.N. McElhaney, Phospholipid phase transitions in model and biological membranes as studied by infrared spectroscopy, Chem. Phys. Lipids 57 (1991) 213–226.
[31] H.L. Casal, H.H. Mantsch, Polymorphic phase behaviour of phospholipid membranes studied by infrared spectroscopy, Biochim. Biophys. Acta 779 (1984) 381–401.
[32] J.H. Crowe, L.M. Crowe, D. Chapman, Infrared spectroscopic studies on interactions of water and carbohydrates with a biological membrane, Arch. Biochem. Biophys. 232 (1984) 400–407.
[33] R.P. Goodrich, J.H. Crowe, L.M. Crowe, J.D. Baldeschwieler, Alterations in membrane surfaces induced by attachment of carbohydrates, Biochemistry 30 (1991) 5313–5318.
[34] V. Luzzati, X-ray diffraction studies of lipid–water systems, in: D. Chapman (Ed.), Biological Membranes, Academic Press, New York, 1968, pp. 71–123.
[35] M. Rappolt, A. Hickel, F. Brigenzu, K. Lohner, Mechanism of the lamellar/inverse hexagonal phase transition examined by high resolution X-ray diffraction, Biophys. J. 84 (2003) 3111–3122.
[36] A. Tardieu, V. Luzzati, F.C. Reman, Structure and polymorphism of the hydrocarbon chains of lipids: a study of lecithin–water phases, J. Mol. Biol. 75 (1973) 711–733.
[37] K. Pressl, K. Jorgenssen, P. Laggner, Characterization of the submain transition in distearoylphosphatidylcholine studied by simultaneous small- and wide-angle X-ray diffraction, Biochim. Biophys. Acta 1325 (1997) 1–7.